Molecular cytogenetics reveals an uncommon structural and numerical chromosomal heteromorphism in *Zephyranthes brachyandra* (Amaryllidaceae)

La citogenética molecular revela un heteromorfismo cromosómico numérico y estructural poco común en *Zephyranthes brachyandra* (Amaryllidaceae)

Thiago Nascimento[1]*, Raquel S. Gonçalves[1], Mariana Báez[1], Guillermo Seijo[2] and Marcelo Guerra[1]

1. Laboratório de Citogenética e Evolução Vegetal, Departamento de Botânica, Universidade Federal de Pernambuco-UFPE, R. Prof. Moraes Rego, s/n, Recife, PE 50670-420, Brazil.
2. Instituto de Botánica del Nordeste (UNNE - CONICET) and Facultad de Ciencias Exactas y Naturales y Agrimensura, Universidad Nacional del Nordeste, Sargento Cabral 2131, 3400 Corrientes, Argentina.

*thiagoagtc@gmail.com

Citar este artículo
NASCIMENTO, T., R. S. GONÇALVES, M. BÁEZ, G. SEIJO AND M. GUERRA. 2022. Molecular cytogenetics reveals an uncommon structural and numerical chromosomal heteromorphism in *Zephyranthes brachyandra* (Amaryllidaceae). *Bol. Soc. Argent. Bot.* 57: 39-49.

DOI: https://doi.org/10.31055/1851.2372.v57.n1.34304

Summary

Background and aims: *Zephyranthes brachyandra* belongs to a tribe of ornamental Amaryllidaceae native of South America, whose genera circumscription and phylogenetic relationships are still unclear. Cytologically, *Z. brachyandra* is a tetraploid whose chromosomes are of similar size and morphology, hindering the identification of its 2*n* = 24 chromosomes. The aim of this study was to investigate the stability of the many CMA$^+$ and DAPI$^+$ bands and the occurrence of B chromosomes by a cytomolecular approach.

M&M: For this investigation we conducted a cytomolecular analysis with CMA/DAPI staining and fluorescence *in situ* hybridization with 5S and 35S rDNA probes, and the TTTAGGG telomeric probe.

Results: In the present work, a cytomolecular analysis of *Z. brachyandra*, revealed a large and variable number of CMA$^+$ and DAPI$^+$ heterochromatic bands and 5S and 35S rDNA sites, and a regular distribution of the TTTAGGG telomeric sequences. In addition, one individual was monotrisomic with 2*n* = 24, and another one had a B chromosome. Both numerical and structural chromosome alterations were clearly characterized by CMA/DAPI bands and rDNA sites.

Conclusions: Comparing the present data with the cytological data for other species of *Zephyranthes*, it becomes clear that a cytomolecular approach is fundamental to the understanding of the chromosome variation and cytotaxonomy of the group.

Key Words

CMA/DAPI banding, cytotaxonomy, FISH, monotrisomy, rDNA, telomeric DNA.

Resumen

Introducción y objetivos: *Zephyranthes brachyandra* pertenece a una tribu de Amaryllidaceae ornamentales nativa de América del Sur, cuya circunscripción de géneros y relaciones filogenéticas aún no están claras. Citológicamente, *Z. brachyandra* es un tetraploide cuyos cromosomas son de tamaño y morfología similar, lo que dificulta la identificación de sus 2*n* = 24 cromosomas. El objetivo de este estudio fue investigar la estabilidad de las numerosas bandas CMA+ y DAPI+ y la aparición de cromosomas B mediante un enfoque citomolecular.

M&M: Para esta investigación realizamos un análisis citomolecular con tinción CMA/DAPI e hibridación fluorescente *in situ* con sondas de ADNr 5S y 35S, y la sonda telomérica TTTAGGG.

Resultados: En el presente trabajo se realizaron varios análisis citomoleculares de *Z. brachyandra*, que revelaron un número alto y variable de bandas heterocromáticas CMA+ y DAPI+ y de sitios de ADNr 5S y 35S, además de una distribución típica de las secuencias teloméricas TTTAGGG. Además, un individuo era monotrisómico con 2*n* = 24 y otro tenía un cromosoma B. Las alteraciones cromosómicas tanto numéricas como estructurales se caracterizaron claramente por bandas CMA / DAPI y sitios de ADNr.

Conclusión: Al comparar los datos actuales con la literatura citológica de otras especies del género *Zephyranthes*, queda claro que un enfoque citomolecular es fundamental para la comprensión de la variación cromosómica y la citotaxonomía del grupo.

Palabras Clave

Bandeamiento CMA/DAPI, citotaxonomía, FISH, monotrisomía, ADNr, ADN telomérico

Recibido: 3 Ago 2021
Aceptado: 18 Feb 2022
Publicado impreso: 31 Mar 2022
Editora: Paola Gaiero

ISSN versión impresa 0373-580X
ISSN versión on-line 1851-2372

Introduction

One of the taxonomic approaches most intensively explored in the last century was cytotaxonomy [summarized by Stebbins (1971)]. The rationale behind this approach is that the karyotype allows a "macroscopic" view of the genetic material of a species, with some particular details of individuals or populations and reveals many characters common to its genus or tribe. In contrast with various other morphological descriptors, karyotype changes, such as polyploidy and chromosome inversions or translocations, may work as reproductive barriers among populations or species, playing therefore an important role in the speciation process (Levin, 2002). Moreover, the karyotype is the only morphological trait that is not affected by gene expression, environmental conditions, age, developmental phase, etc (Guerra, 2012). In general, using appropriate techniques, karyotype similarity among species of a genus is an indicative of their phylogenetic proximity.

Karyotype description was initially restricted to chromosome number, size and morphology (Stebbins, 1971), but recent advances on molecular cytogenetics expanded the number of chromosomal marks and allowed a more detailed karyotype description (Jiang, 2019). For example, the chromosomes of all species of *Citrus* and related genera are very similar in number, size and morphology but they differ widely in the number and distribution of heterochromatic bands and 5S and 35S rDNA sites (reviewed by Guerra, 2009). Likewise, the assumption that the families Juncaceae and Cyperaceae had holocentric chromosomes as one of their synapomorphies (Judd *et al*., 2016) was overturned by careful analyses of the chromosome morphology and centromere immunostaining of some *Juncus* species, revealing that in Juncaceae, at least, holocentricity is rather a particularity of a few genera (Guerra *et al*., 2019).

Structural chromosome differentiation is most commonly revealed by identification of heterochromatic bands and sites of highly conserved DNA sequences, as the telomeric DNA and 5S and 35S rRNA genes. These marks are composed by repetitive DNA sequences densely concentrated into a few blocks and located preferentially at the centromeric and terminal chromosome regions or near the nucleolus organizer region (Guerra, 2000; Roa & Guerra, 2015; Samoluk *et al.,* 2017). Within certain limits, the amount of heterochromatin is not critical to genome function but in a few species it is enormously expanded, forming large heterochromatic blocks, as in *Trithrinax campestris* and *Capsicum* species (Gaiero *et al*., 2012; Grabiele *et al.,* 2018), or numerous small bands, as in *Cuscuta monogyna* (Ibiapino *et al*., 2020). The tandemly repeated nature of rDNA and telomeric DNA sites allows a considerable variation in number and size of these sites, contributing to a better karyotype characterization of species or populations (Pedrosa-Harand *et al*., 2006; Robledo & Seijo, 2010; Rosato *et al*., 2017, 2018; Silvestri *et al*., 2020). Currently, chromosome staining with the fluorochromes chromomycin A_3 (CMA) and 4',6-diamidino-2-phenylindole (DAPI) is the most used method to differentiate GC-rich and AT-rich heterochromatic bands, respectively (Guerra, 2000). Other more specific chromosome regions are revealed by fluorescence *in situ* hybridization (FISH), a well stablished method to localize any type of DNA sequence along the chromosomes (Jiang, 2019). The analysis of CMA/DAPI bands and rDNA sites, or other DNA sequences revealed by FISH, into a phylogenetic context has ensured an enormous progress in cytotaxonomical analyses (e.g., Chalup *et al*., 2015; Silvestri *et al.,* 2020; Ribeiro *et al*., 2020). However, cytomolecular methods are more time-consuming and have been used in a still limited number of cytotaxonomical works.

Zephyranthes brachyandra (Baker) Backer (Amaryllidaceae) is an ornamental bulbous plant native of the Neotropics, from southern South America to Mexico and southwest USA, including southern Brazil and West Indies, sometimes referred to as *Habranthus brachyandrus* (Baker) Sealy (Daviña, 2001; Daviña & Honfi, 2018; García *et al*. 2019). Phylogenetically, the former genera *Zephyranthes* and *Habranthus* are now recognized as subgenera of *Zephyranthes* s.l. (García *et al*. 2019). The two subgenera share similar chromosome size and morphology, large variation in chromosome numbers, mainly with $x = 6$, several ploidy levels, and some species with B chromosomes (Naranjo, 1974; Felix *et al.,* 2008, 2011a; Daviña, 2001; Daviña & Honfi, 2018).

Cytologically, *Z. brachyandra* is a tetraploid with $2n = 24$, characterized by many $DAPI^+$ and CMA^+ heterochromatic bands located in the interstitial-terminal region of most chromosome arms (Felix *et al*., 2011b). The individual analyzed by Felix *et al*. (2011b) presented $2n = 24$ plus one B chromosome, whereas the five bulbs examined by Daviña (2001) exhibited always $2n = 24$. B chromosomes are extra chromosome usually smaller than the regular chromosomes of the species (A chromosomes), mostly depleted of genes, and present only in some individuals of the species (see, *e.g*., Marques *et al*., 2013; Vanzela *et al*., 2017). They may occasionally be accumulated in some individuals affecting their DNA content and some other phenotype characters (Huang *et al*., 2016).

In the present work, we conducted a detailed karyotype analysis of three individuals of *Z. brachyandra* collected in the field, aiming to investigate: a, the stability of the many CMA^+ and $DAPI^+$ bands reported previously for a single individual *(*Felix *et al*. 2011b); b, the distribution of 5S rDNA, 35S rDNA and telomeric DNA sites; c, the occurrence of B chromosomes. We also evaluated karyotype similarity in chromosome number, size and morphology, banding patterns and rDNA sites of *Z. brachiandra* with other species of the genus*,* in order to contribute to the cytotaxonomy of *Zephyranthes*.

Material and Methods

Plants material

Three bulbs of *Z. brachyandra* were collected in San Javier (27º52´17.9´´- 55º07´41.7´´), Misiones, Argentina, and cultivated in the Experimental Garden of the Department of Botany, Federal University of Pernambuco, Recife, Brazil. A voucher was deposited in the herbarium Prof. Jayme Coelho de Moraes (Federal University of Paraiba, Brazil, voucher EAN 29460).

Slides preparation

For mitotic analyses, young root tips were pretreated with colchicine 0.2% at 10 °C for 24 h, fixed in ethanol-acetic acid (3:1, v/v) for 2 h at room temperature, then stored at –20 °C until the moment of use. The fixed meristems were washed twice in destilled water, digested in a 2% cellulase (Onozuka)/ 20% pectinase (Sigma) solution at 37 °C for one hour, and macerated in a drop of 45% acetic acid. The coverslips were removed in liquid nitrogen and the slides were dried in the air. The preparations were mounted and stained with a 1 µg/mL DAPI/glycerol (1:1) solution, in order to select the best slides. Subsequently, they were destained in ethanol/acetic acid (3:1), air dried, and aged for three days at room temperature.

Chromosome staining with CMA/DAPI and FISH

Chromosome double staining with the fluorochromes CMA (Sigma) and DAPI (Sigma) was performed as described by Vaio *et al.* (2018). Aged slides were stained with CMA (0.1 mg/mL) for 1 h, counterstained with DAPI (2 µg/mL), mounted with glycerol-McIlvaine buffer pH 7.0 (1:1) and aged again for three days. After image capture of the best metaphases the chromosomes were destained and *in situ* hybridized according to Pedrosa *et al*. (2002). The probes used for 5S and 35S rDNA sites were, respectively, D2 from *Lotus japonicus* (Regel) K. Larsen and a clone from *Triticum aestivum* L. (plasmid Pta71). The probes were direct and indirect labeled with Cy3 dUTP (GE Healthcare) (5S rDNA probe) and digoxigenin-11-dUTP (Roche) (35S rDNA probe) respectively, both by nick translation (Invitrogen). The hybridization mixture contained 50% formamide (v/v), 10% dextran sulfate (w/v), 2x SSC, and 5–10 ng/µL of rDNA probe, accomplishing a final stringency of ~76%. The 35S rDNA probe was detected with sheep anti-digoxigenin–FITC (Roche).

For detection of telomeric sites, a synthetic TTTAGGG oligoprobe labeled with Cy3 by Macrogen Inc. was *in situ* hybridized according to the protocol of Cuadrado *et al*. (2010), slightly modified. Briefly, 10 µL of the probe solution (8 ng/µL of the oligoprobe diluted in 2x SSC) were applied to each slide for 2 h at room temperature. Afterwards, the slides were washed in 4x SSC/0.2% Tween20 for 10 min. All preparations were counterstained and mounted with 2 µg/mL DAPI in Vectashield (Vector). Images of the best cells were captured with a Leica DM5500B fluorescence microscope and later processed with Adobe Photoshop CC 2020 for brightness, contrast, and sharpness.

Chromosome measurements

In order to characterize chromosome size and morphology, chromosomes of the three best metaphases for each karyotype were measured using the software DRAWID version 0.26 (Kirov *et al*., 2017). The chromosome arm ratio [*r* = length of long arm (*l*)/short arm (*s*)] was used to define chromosomes as metacentric (*r* = 1.0-1.49), submetacentric (*r* = 1.50-2.99), acrocentric (AR ≥ 3.0) or telocentric, according to Guerra (1986). Chromosome pairs were ordered from I to XII by decreasing size of the short arm.

Results

The plants collected in Argentina grew very well and flowered during the summer in Recife (Fig. 1), but only produced sterile seeds. They revealed a high rate of asexual reproduction by lateral bulb production, providing plenty of material for investigation. About 15 metaphases of each individual were analyzed for chromosome number. Two individuals analyzed presented $2n = 24$ and a third presented $2n = 24$ plus a B chromosome. The three best metaphases of each plant were selected for a careful comparison of CMA/DAPI bands and rDNA sites. Two karyograms were mounted for each individual and a single ideogram was constructed summarizing the average sizes for each chromosome pair and heterochromatic bands and rDNA sites common to all of them (Fig. 2). The individuals without B chromosomes were heteromorphic for a chromosome pair formed by a meta- and a submetacentric chromosome and were karyotypically identical regarding all other chromosome characteristics, suggesting that they were clones from a single individual. Therefore, they will be referred to herein as a single karyotype. Excluding the B chromosome, chromosome size varied from 14.59 to 9.28 µm and the average haploid complement size was 146.75 µm (Fig. 2 and Table 1). The chromosome morphology in the two karyotypes was very similar, except for the arm ratio of chromosome pair X, which was 1.24 for the karyotype without B and 1.80 for the karyotype with B. This difference changed its chromosome morphology from metacentric (AR = 1.00-1.49) to submetacentric (AR = 1.50-2.99) (Guerra, 1986) and the karyotype formula from 8M + 4SM for the individual with $2n = 24$ to 9M + 3SM for the individual with $2n = 24 + 1B$ (the chromosome B was not included in the karyotype formula). The average arm ratio for pair X considering both karyotypes was 1.52 (Fig.2). The remaining chromosomes were metacentrics (pairs I to IX) or submetacentrics (pairs XI and XII). The most outstanding karyotype feature of *Z. brachyandra* was the large amount of $DAPI^+$ heterochromatin. There were large $DAPI^+$ bands on the short arm of 10 chromosomes and one to four small bands in the interstitial/terminal region of the remaining chromosome arms (Fig. 3A). The submetacentric pairs XI and XII presented similar size and morphology, differing mainly in the number of $DAPI^+$ bands on the long arm: two on pair XI and three on pair XII. CMA^+ bands were identified only in the short arms of the smaller submetacentrics (Fig. 3A') and in the short arm of pair VIII (not always visible). Besides these general features, the two karyotypes observed here had several small structural differences.

The number and position of the 5S and 35S rDNA loci complemented the identification of each chromosome pair and were different in the two karyotypes. The karyotype with the heteromorphic pair had 19 sites of 5S and six sites of 35S rDNA. The 5S rDNA sites were located on the interstitial (12 sites) or terminal (7 sites) regions of the large metacentric and

Fig. 1. Flowers of *Zephyranthes brachyandra* cultivated as ornamental plants in Recife, Brazil.

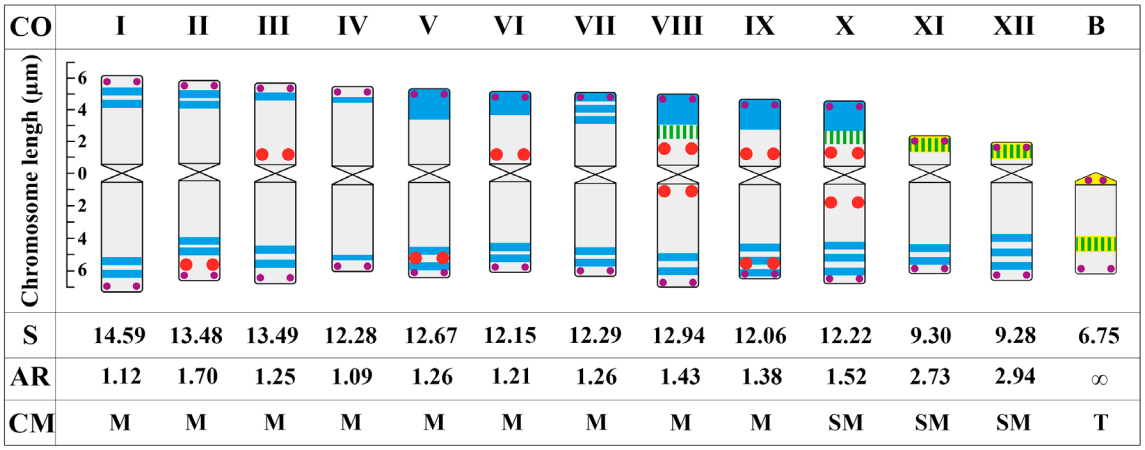

Fig. 2. Idiogram of *Z. brachyandra,* including all characters observed in both karyotypes plus the B chromosome. CO, chromosome order; S, chromosome size in µm; AR, arm ratio; CM, chromosome morphology. The scale on the left side indicates the size of the chromosome arms. Blue = DAPI$^+$ band; yellow = CMA$^+$ band; yellow with green bars = 35S rDNA sites co-localized with CMA+ bands; red dots = 5S rDNA sites; very small purple dots = TTTAGGG sites.

Table 1. Chromosome data of *Zephyranthes brachyandra* karyotype, including chromosome order (CO, larger to smaller short arm), short and long arm sizes, chromosome size, arm ratio, chromosome morphology (CM), number and position of DAPI+ bands and CMA+ bands, and number and position of 5S and 35S rDNA sites. DAPI+ bands were classified as large (L) or small (S), CMA+ bands as terminal (T), and rDNA sites as terminal (T) or interstitial (i). Chromosomal marks on the short arms are superscript and those on the long arms are subscript.

CO	Short arm (µm)	Long arm (µm)	Chromosome Size (µm)	Arm ratio	CM	DAPI bands	CMA bands	5S rDNA sites	35S rDNA sites
I	6.91 ± 0.98	7.68 ± 0.92	14.59 ± 1.82	1.12 ± 0.09	M	$2^S + 2_S$	--	--	--
II	6.20 ± 0.78	7.28 ± 1.27	13.48 ± 1.97	1.70 ± 0.12	M	$2^S + 2_S$	--	1^T	--
III	6.06 ± 1.13	7.42 ± 0.98	13.49 ± 1.88	1.25 ± 0.23	M	$1^S + 2_S$	--	--	--
IV*	5.89 ± 0.92	6.39 ± 0.92	12.28 ± 1.83	1.09 ± 0.06	M	$1^S + 1_S$	--	--	--
IV*	2.58 ± 0.23	7.33 ± 0.31	9.91 ± 0.42	2.87 ± 0.34	SM	$2^S + 2_S$	1^T	--	1^T
V	5.65 ± 0.63	7.02 ± 0.65	12.67 ± 0.98	1.26 ± 0.19	M	$1^L + 2_S$	--	1^T	--
VI	5.49 ± 0.56	6.65 ± 0.85	12.15 ± 1.28	1.21 ± 0.13	M	$1^L + 2_S$	--	1^i	--
VII	5.44 ± 0.68	6.84 ± 0.85	12.29 ± 1.45	1.26 ± 0.09	M	$3^S + 2_S$	--	--	--
VIII	5.40 ± 0.95	7.54 ± 1.21	12.94 ± 1.93	1.43 ± 0.32	M	$1^L + 2_S$	--	$1^i + 1_i$	1^i
IX	5.10 ± 0.60	6.95 ± 0.95	12.06 ± 1.21	1.38 ± 0.24	M	$1^L + 3_S$	--	$1^i + 1_T$	--
X	4.93 ± 0.95	7.29 ± 1.23	12.22 ± 1.77	1.52 ± 0.34	SM	$1^L + 3_S$	--	$1^i + 1_i$	1^i
XI	2.52 ± 0.38	6.78 ± 0.75	9.30 ± 0.93	2.73 ± 0.41	SM	2_S	1^T	--	1^T
XII	2.09 ± 0.28	7.19 ± 0.94	9.28 ± 0.96	2.94 ± 0.87	SM	3_S	1^T	--	1^T
B	--	6.75 ± 0.45	6.75 ± 0.45	∞	A	--	$1^T + 1_T$	--	1_T

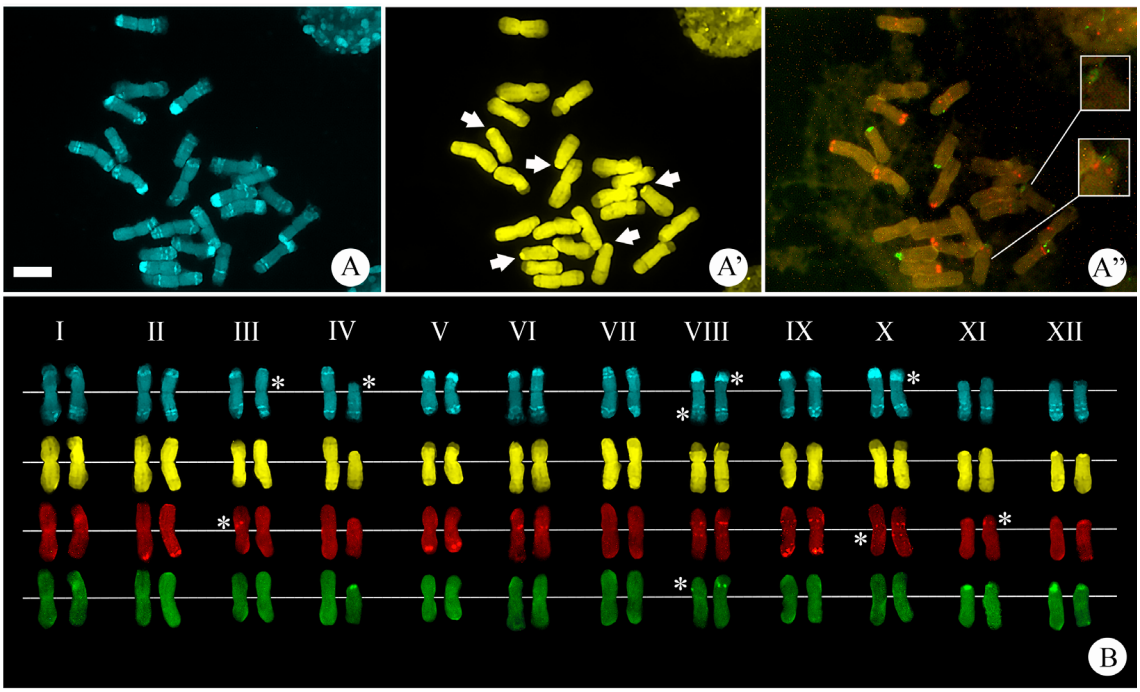

Fig. 3. Metaphase of *Z. brachyandra* with a heteromorphic chromosome pair. Chromosomes were stained with DAPI (**A**) and CMA (**A'**) and *in situ* hybridized with 5S (red) and 35S (green) rDNA probes (**A"**). Arrows in **A'** point to CMA$^+$ bands of submetacentrics. Inset in **A"** shows magnified images of small rDNA sites. Karyograms based on this metaphase allow the identification of each chromosome pair by comparison of the different marks (**B**). Asterisks in **B** indicate heteromorphic pairs. Bar in **A** corresponds to 10 µm.

submetacentric chromosomes and a single site on one homologue of pair XI (Fig 3A''). The five small submetacentrics had a 35S rDNA site on the short arm co-localized with the CMA$^+$ band. One chromosome of pair VIII also displayed a small 35S rDNA near the large DAPI$^+$ band, but it was not co-localized with a CMA$^+$ band. The karyograms based on Fig. 3A-A'' placed the extra small submetacentric provisionally as pair IV (Fig. 3B), since one homologue of pair IV was absent. However, it was almost identical to pair XI in size and morphology as well as in banding patterns, with two weakly differentiated DAPI$^+$ bands on the long arm and a CMA$^+$ band on the short one. At least six other chromosome pairs were heteromorphic for one or more bands or sites (asterisks in figure 3B).

The karyotype with a B chromosome exhibited a similar pattern of CMA/DAPI bands and rDNA sites (Fig. 4A-A'). It had 19 sites of 5S rDNA, including an extra signal on the short arm of both homologues of pair V and a heteromorphic site on pair X, and 12 sites of 35S rDNA plus one in the B chromosome. Noteworthy, the additional 35S rDNA sites, located on pairs VIII and X, were not clearly detected as CMA+ bands. The 35S rDNA site on pair X was very close to the large DAPI$^+$ band but they were not colocalized (see insets in Fig. 4A and respective chromosomes in Fig. 4B).

The TTTAGGG probe labelled the telomeric regions of all chromosomes of both karyotypes and no ectopic site was found (Fig. 5). No short arm was visible on the B chromosome, suggesting that it was a telocentric. It was shorter (6.75 µm) than the submetacentrics (Fig. 2), had no DAPI$^+$ bands, and presented two CMA$^+$ bands: one interstitial and one very small on its narrower end (inset in Fig. 4A'). The latter could be the centromere itself or a very small short arm, whereas the interstitial band coincided with a 35S rDNA site.

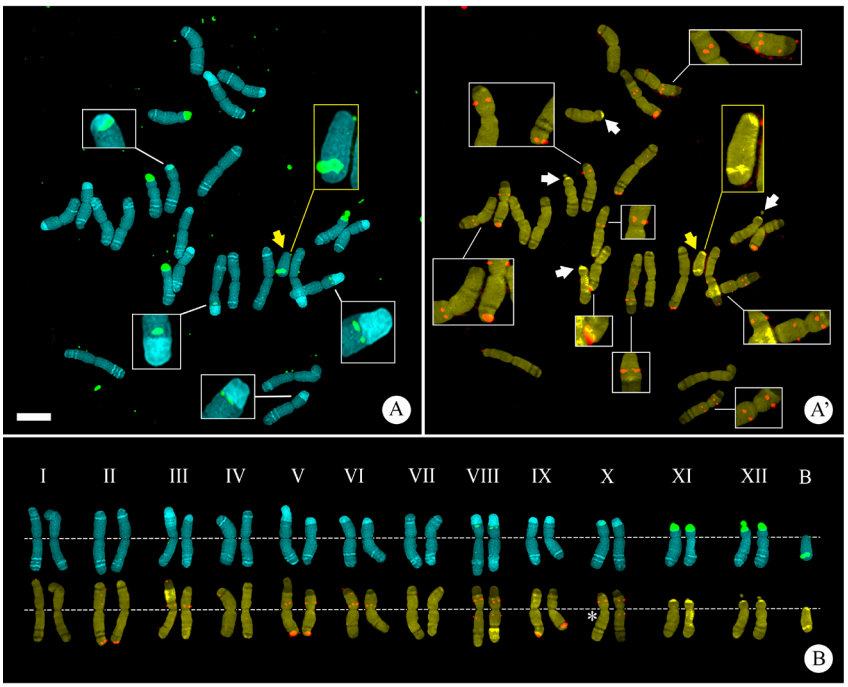

Fig. 4. Metaphase of *Z. brachyandra* with 2*n* = 24 + 1B displaying DAPI$^+$ bands (blue) plus 35S rDNA sites (green) (**A**) and CMA$^+$ bands (white arrows) plus 5S rDNA sites (red dots) (**A'**). Insets show magnified chromosome regions with small rDNA sites (white frames) and B chromosome (yellow arrows and frames). Karyograms (**B**) were based on the same metaphase. Bar in **A** corresponds to 10 µm.

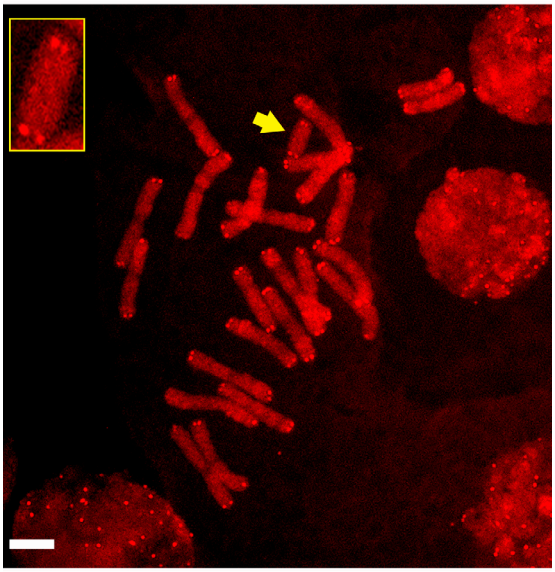

Fig. 5. *In situ* hybridization of the TTTAGGG probe in a metaphase of *Z. brachyandra* with 2*n* = 24 + 1B (arrow) revealed terminal sites only. Inset shows magnified B chromosome. Bar corresponds to 10 µm.

Discussion

The two karyotypes of *Z. brachyandra* analysed here differed mainly in the occurrence of a heteromorphic chromosome pair in one of them and a B chromosome in the other. Regarding chromosome sizes and haploid karyotype formula, our data (14.59 to 9.28 µm and 8M + 4SM or 9M + 3SM) differ in part from that reported by Daviña (2001) (10.89 to 6.14 µm and 8M + 4SM). The difference in chromosome size may be due to the distinct anti-mitotic pre-treatment and the condensation status of selected metaphases (Guerra, 2012), whereas the karyotype formula 8M + 4SM was the same found here for the karyotype without B. Therefore, in spite of the small sample size, our data revealed karyotype instability, which was not detected in previous studies.

The two karyotypes displayed a similar number of CMA/DAPI bands and differed slightly in the number of the 5S and 35S rDNA sites. The complex DAPI$^+$ banding pattern of *Z. brachyandra* was

similar to that reported by Felix *et al.* (2011b), while the number and position of CMA^+ bands reported by these authors were quite distinct from the present ones. They found eight or ten bright CMA^+ bands (excepting the B chromosome), only two of them on small submetacentric chromosomes, whereas in our sample there were only four or six CMA^+ bands (excepting the B and the extra submetacentric chromosome). It is possible that some CMA^+ bands in our sample had not been detected because they were too small. Actually, the 35S rDNA sites of pairs VIII and X were expected to be CMA^+, since they are usually co-localized with CMA^+ bands (e.g., Moraes *et al.,* 2007; Gaiero *et al*., 2012; Silva *et al.,* 2019). However, small rDNA sites, like those, are sometimes not detected as CMA^+ bands (e.g., Vaio *et al*., 2018). Variation in size and number of heterochromatic bands and rDNA sites depends on the number of repetitive sequences per locus, which may be caused by recombination events with unequal exchanges (Lower *et al*., 2018). However, the position of some interstitial CMA^+ bands reported by Felix *et al.* (2011b) did not coincide with position of the 35S rDNA sites found in our sample, suggesting that if they correspond to 35S rDNA sites, they are not the same reported here.

B chromosomes probably arise from regular A chromosomes and can alter their original DNA composition by rapidly accumulating or losing several DNA sequences (Marques *et al*., 2013). In *Z. brachyandra* the only B chromosome observed was a telocentric chromosome similar in size and morphology to that reported by Felix *et al.* (2011a,b), but without the two interstitial $DAPI^+$ bands observed by those authors. Both Bs had a small terminal CMA^+ band, although only one reported here had an extra interstitial CMA^+ band co-localized with a 35S rDNA site. Polymorphisms on B chromosomes are more common than in the regular chromosomes, probably due to the dispensable nature of Bs (Marques *et al*., 2013; Vanzela *et al*., 2017).

At first sight, the extra submetacentric chromosome found in a karyotype with the normal chromosome number seemed to be a partial deletion of the short arm of a metacentric chromosome. Heteromorphism for large chromosome segments are rare but have already been clearly documented for several plant species, especially those with large chromosomes, as *Crocus cancellatus* (Brighton, 1976) and *Alloe rabaiensis* (Bradham, 1983). However, the similarity of the extra submetacentric with chromosome pair XI in size, morphology, and CMA/DAPI bands, as well as the absence of one homologue of pair IV, suggest that this karyotype had a trisomy for pair XI combined and a monosomy for pair IV. Such monotrisomic aneuploids are more commonly found among chromosomically engineered crop plants, as wheat and barley, and most of them are compensating aneuploids involving homeologous chromosomes (Singh, 2003). Differently, in *Z. brachyandra* the monotrisomy involved two quite different chromosomes, although the plant phenotype was identical to the normal plants. In this case, the normal appearance of the individual is most probably due to the buffer effect of polyploidy, in which a deletion or a duplication of an entire chromosome of a tetraploid genome could not be sufficient to alter the phenotype (Deng *et al*., 2018). The occurrence of aneuploid plants is more common in meiotically instable polyploids (Mandáková & Lysak, 2018), while *Z. brachyandra* has a regular meiosis (Daviña, 2001; Daviña & Honfi, 2018). Monotrisomy in wild plants has rarely been reported, but it is probably underestimated because its detection demands a clear distinction of the chromosomes involved, as demonstrated in *Tragopogon miscellus* (Chester *et al*., 2012) and *Nothoschordum bonariense* (Souza *et al*., 2019). Trisomy as well as B chromosomes have also been reported in some other species of *Zephyranthes* (see e.g., Felix *et al*., 2008, 2011a,b).

Despite the polymorphisms observed here, *Z. brachyandra* is karyotypically very well defined, due to its many chromosome marks. The only other *Zephyranthes* species where rDNA sites have been investigated is *Z. robusta*, a diploid with $2n = 12$ (10M + 2SM) and similar chromosome sizes. The molecular karyotype of *Z. robusta* is also similar to that expected for a hypothetical diploid ancestor of *Z. brachyanda,* with two 35S rDNA sites co-localized with CMA^+ bands on submetacentric short arms, ten 5S rDNA sites, some interstitial and subterminal $DAPI^+$ bands and a few other heterochromatic blocks detected by C-banding (Barros e Silva & Guerra, 2010; Felix *et al*., 2011b; A.E. Barros e Silva, unpublished results). This similarity points to a possible autopolyploid origin for *Z. brachiandra*, in spite of its regular meiotic pairing (Daviña and Honfi, 2018), which

is usually associated with allopolyploidy. Regular bivalent formation has also been reported for other autopolyploids, as *Arabidopsis arenosa* (Carvalho *et al*., 2010), and autopolyploidy may be not as rare as supposed earlier (Soltis *et al*., 2007). The assumption of an autopolyploid origin for *Z. brachiandra* could also explain the many duplicated patterns of chromosome banding and rDNA site distribution observed here, some of them blurred by the intense heteromorphism characteristic of heterochromatic bands and rDNA sites (Chalup *et al*., 2015; Silvestri *et al.,* 2020; Ribeiro *et al*., 2021). Five other species of *Zephyranthes* analysed by Felix *et al*. (2011b) revealed a much smaller and variable number of CMA^+ bands and no $DAPI^+$ bands, suggesting that a cytomolecular investigation of other *Zephyranthes* species would be very helpful to understand the cytotaxonomy and chromosomal evolution of this group.

Authors Contribution

THN conducted the FISH experiments, analyzed the data, constructed the figures and tables and wrote the paper. RSG conducted FISH experiments and helped to write the paper. MB collected the material, conducted FISH experiments and helped to write the paper. GS collected the material and helped to write the paper. MG discussed the results, provided resources for the FISH experiments, designed this research and wrote the paper. All authors read and approved the final version of the paper.

Bibliography

BARROS E SILVA, A. E. & M. GUERRA. 2010. The meaning of DAPI bands observed after C-banding and FISH procedures. *Biotech. Histochem*. 85: 115–125. https://doi.org/10.3109/10520290903149596

BRADHAM, P. 1983. Evolution in a stable chromosome system. In: P.E. BRADHAM & M.D. BENNET (Eds). George Allen & Unwin (Publishers), *Kew Chromosome Conference II*, pp. 251-260. London.

BRIGHTON, C. A. 1977. Cytological problems in the genus *Crocus* (Iridaceae): II. *Crocus Cancellatus* Aggregate. *Kew Bulletin* 32: 33-45. https://doi.org/10.2307/4117257

CARVALHO A., M. DELGADO, A. BARÃO, M. FRESCATADA, E. RIBEIRO, C. S. PIKAARD, W. VIEGAS & N. NEVES. 2010. Chromosome and DNA methylation dynamics during meiosis in the autotetraploid *Arabidopsis arenosa*. *Sex. Plant. Reprod*. 23:29-37. https://doi.org/10.1007/s00497-009-0115-2

CHALUP, L., S. S. SAMOLUK, V. S. NEFFA & G. SEIJO. 2015. Karyotype characterization and evolution in South American species of *Lathyrus* (Notolathyrus, Leguminosae) evidenced by heterochromatin and rDNA mapping. *J. Plant Res.* 128: 893–908. https://doi.org/10.1007/s10265-015-0756-1

CHESTER, M., J. P. GALLAGHER, V. V. SYMONDS, A. V. C. SILVA, E. V. MAVRODIEV, A. R. LEITGH, P. S. SOLTIS & D. E. SOLTIS. 2012. Extensive chromosomal variation in a recently formed natural allopolyploid species, *Tragopogon miscellus* (Asteraceae). *Proc. Natl. Acad. Sci.* 109: 1176–1181. https://doi.org/10.1073/pnas.1112041109

CUADRADO, A. & N. JOUVE. 2010. Chromosomal detection of Simple Sequence Repeats (SSRs) using nondenaturing FISH (ND-FISH). *Chromosoma* 119: 495–503. https://doi.org/10.1007/s00412-010-0273-x

DAVIÑA, J. R. 2001. *Estudios citogenéticos en algunos géneros argentinos de Amaryllidaceae*. Doctoral thesis, Universidade Nacional de Córdoba, Córdoba, Argentina.

DAVIÑA, J. R. & A. I. HONFI. 2018. IAPT chromosome data 28 [extended online version]. In: MARHOLD K. AND KUČERA J. (Eds.). *Taxon.* 67: E1–E46. https://doi.org/10.12705/676.39

DENG, X., Y. SHA, Z. LV, Y. WU, A. ZHANG, F. WANG & B. LIU. 2018. The capacity to buffer and sustain imbalanced D-subgenome chromosomes by the BBAA component of hexaploid wheat is an evolved dominant trait. *Front. Plant Sci.* 9: 1–12. https://doi.org/10.3389/fpls.2018.01149

FELIX, W. J. P., J. H. A. DUTILH, N. F. M., ANDREA A. F. & LEONARDO P. F. 2008. Intrapopulational chromosome number variation in *Zephyranthes sylvatica* Baker (Amaryllidaceae: Hippeastreae) from Northeast Brazil. *Rev. Bras. Bot.* 31: 371–75. https://doi.org/10.1590/S0100-84042008000200020

FELIX, W. J. P., L. P. FELIX, N. F. MELO, M. B. M. OLIVEIRA, J. H. A. DUTILH & R. CARVALHO. 2011a. Karyotype variability in species of the genus *Zephyranthes* Herb. (Amaryllidaceae–Hippeastreae). *Plant Syst. Evol.* 294**:** 263. https://doi.org/10.1007/s00606-011-0467-6

FELIX, W. J. P., L. P. FELIX, N. F. MELO, J. H. A. DUTILH & R. CARVALHO. 2011b. Cytogenetics of Amaryllidaceae species: heterochromatin evolution in different ploidy levels. *Plant Syst. Evol.* 292: 215–221. https://doi.org/10.1007/s00606-011-0418-2

GAIERO, P., C. MAZZELLA, M. VAIO, A. E. BARROS E SILVA, F. F. SANTIÑAQUE, B. LÓPEZ-CARRO, G. A. FOLLE & M. GUERRA. 2012. An unusually high heterochromatin content and large genome size in the palm tree *Trithrinax campestris* (Arecaceae). *Aust. J. Bot.* 60: 378. http://dx.doi.org/10.1071/BT12029

GARCÍA N., A. W. MEEROW, S. ARROYO-LEUENBERGER, R. S. OLIVEIRA, J. H. DUTILH, P. S. SOLTIS & W. S. JUDD. 2019. Generic classification of Amaryllidaceae tribe Hippeastreae. *Taxon* 68: 481-498. https://doi.org/10.1002/tax.12062

GRABIELE, M., H. J. DEBAT, M. A. SCALDAFERRO, P. M. AGUILERA, E. A. MOSCONE, J. G. SEIJO & D. A. DUCASSE. 2018. Highly GC-rich heterochromatin in chili peppers (*Capsicum*-Solanaceae): A cytogenetic and molecular characterization. *Sci. Hortic.* 238: 391–399. https://doi.org/10.1016/j.scienta.2018.04.060

GUERRA, M. S. 1986. Reviewing the chromosome nomenclature of Levan *et al. Braz. J. Genet.* 9: 741-743.

GUERRA, M. 2000. Patterns of heterochromatin distribution in plant chromosomes. *Genet. Mol. Biol.* 23: 1029–1041. https://doi.org/10.1590/S1415-47572000000400049

GUERRA, M. 2009. Chromosomal variability and the origin of *Citrus* species. In: Mahoney C. L. & Springer D. A. (Eds) *Genetic diversity,* pp. 51-68., Nova Science Publishers New York..

GUERRA, M. 2012. Cytotaxonomy: the end of childhood. *Plant Biosyst.* 146: 703–710. https://doi.org/10.1080/11263504.2012.717973

GUERRA, M., T. RIBEIRO & L. P. FELIX. 2019. Monocentric chromosomes in *Juncus* (Juncaceae) and implications for the chromosome evolution of the family. *Bot. J. Linn. Soc.* 191: 475-483. https://doi.org/10.1093/botlinnean/boz065

HUANG, W., Y. DU, X. ZHAO & W. JIN. 2016. B chromosome contains active genes and impacts the transcription of A chromosomes in maize (*Zea mays* L.). *BMC Plant Biol.* 16: 88. https://doi.org/10.1186/s12870-016-0775-7

IBIAPINO, A., M. A. GARCÍA, M. COSTEA, S. STEFANOVIĆ & M. GUERRA. 2020. Intense proliferation of rDNA sites and heterochromatic bands in two distantly related *Cuscuta* species (Convolvulaceae) with very large genomes and symmetric karyotypes. *Genet. Mol. Biol.* 43: 1–9. https://doi.org/10.1590/1678-4685-GMB-2019-0068

JIANG, J. 2019. Fluorescence *in situ* hybridization in plants: recent developments and future applications. *Chromosome Res.* 27: 153–165. https://doi.org/10.1007/s10577-019-09607-z

JUDD, W. S., CAMPBELL C. S., KELLOGG E. A., STEVENS P. F. & DONOGHUE M. J. 2016. *Plant systematics: a phylogenetic approach*. 4th ed. Sunderland, Sinauer Associates.

KIROV, I., L. KHRUSTALEVA, K. V. LAERE, A. SOLOVIEV, S. MEEUS, D. ROMANOV & I. FESENKO. 2017. DRAWID: user-friendly java software for chromosome measurements and idiogram drawing. *Comp. Cytogenet.* 11: 747–757. https://doi.org/10.3897/compcytogen.v11i4.20830

LEVIN, D. A. 2002. *The role of chromosomal change in plant evolution.* New York, Oxford University Press.

LOWER, S. S., M. P. MCGURK, A. G. CLARK & D. A. BARBASH. 2018. Satellite DNA evolution: old ideas, new approaches. *Curr. Opin. Genet. Dev.* 49: 70–78. https://doi.org/10.1016/j.gde.2018.03.003

MANDÁKOVÁ, T. & M. A. LYSAK. 2018. Post-polyploid diploidization and diversification through dysploid changes. *Curr. Opin. Plant Biol.* 42: 55–65. https://doi.org/10.1016/j.pbi.2018.03.001

MARQUES, A., A. M. BANAEI-MOGHADDAM, S. KLEMME, F. R. BLATTNER, K. NIWA, M. GUERRA & A. HOUBEN. 2013. B chromosomes of rye are highly conserved and accompanied the development of early agriculture. *Ann. Bot.* 112: 527–534. https://doi.org/10.1093/aob/mct121

MORAES, A. P., R. R. LEMOS, A. C. BRASILEIRO-VIDAL, W. S. S FILHO & M. GUERRA. 2007. Chromosomal markers distinguish hybrids and non-hybrid accessions of mandarin. *Cytogenet. Genome Res.* 119: 275–281. https://doi.org/10.1159/000112074

NARANJO, C. A. 1974. Karyotypes of four argentine species of *Habranthus* and *Zephyranthes* (Amaryllidaceae). *Phyton*. 32: 61–71.

PEDROSA, A., N. SANDAL, J. STOUGAARD, D. SCHWEIZER & A. BACHMAIR. 2002. Chromosomal map of the model legume *Lotus japonicus. Genetics* 161:1661-1672.

PEDROSA-HARAND, A., C. C. S. ALMEIDA, M. MOSIOLEK, M. W. BLAIR, D. SCHWEIZER & M. GUERRA. 2006. Extensive ribosomal DNA amplification during Andean common bean (*Phaseolus vulgaris* L.) evolution. *Theor. Appl. Genet.* 112: 924–933. https://doi.org/10.1007/s00122-005-0196-8

RIBEIRO, T., E. VASCONCELOS, K. G. B. SANTOS, M. VAIO, A.C. BRASILEIRO-VIDAL & A. PEDROSA-HARAND. 2020. Diversity of repetitive sequences within compact genomes of *Phaseolus* L. beans and allied genera *Cajanus* L. and *Vigna* Savi. *Chromosome Res.* 28: 139–153. https://doi.org/10.1007/s10577-019-09618-w

RIBEIRO, T., J. NASCIMENTO, A. SANTOS, L. P. FÉLIX, & M. GUERRA. 2021. Origin and evolution of highly polymorphic rDNA sites in *Alstroemeria longistaminea* (Alstroemeriaceae) and selated species. *Genome* 64: 833–45. https://doi.org/10.1139/gen-2020-0159

ROA, F. & M. GUERRA. 2015. Non-random distribution of 5S rDNA sites and its association with 45S rDNA in plant chromosomes. *Cytogenet. Genome Res.* 146: 243–249. https://doi.org/10.1159/000440930

ROBLEDO, G. & G. SEIJO. 2010. Species relationships among the wild non-B genome of *Arachis* species (section *Arachis*) based on FISH mapping of rDNA loci and heterochromatin detection: a new proposal for genome arrangement. *Theor. Appl. Genet.* 121: 1033–1046. https://doi.org/10.1007/s00122-010-1369-7

ROSATO, M., I. ÁLVAREZ, G. N. FELINER & J. A. ROSSELLÓ. 2017. High and uneven levels of 45S rDNA site-number variation across wild populations of a diploid plant genus (*Anacyclus*, Asteraceae). *PLoS One* 12: e0187131. https://doi.org/10.1371/journal.pone.0187131

ROSATO, M., I. ÁLVAREZ, G. N. FELINER & J. A. ROSSELLÓ. 2018. Inter- and intraspecific hypervariability in interstitial telomeric-like repeats (TTTAGGG)n in *Anacyclus* (Asteraceae). *Ann. Bot.* 122: 387–395. https://doi.org/10.1093/aob/mcy079

SAMOLUK, S. S., L. M. I. CHALUP, C. CHAVARRO, G. ROBLEDO, D. J. BERTIOLI, S. A. JACKSON & J. G. SEIJO. 2019. Heterochromatin evolution in *Arachis* investigated through genome-wide analysis of repetitive DNA. *Planta* 49: 1405-1415. https://doi.org/10.1007/s00425-019-03096-4

SILVA, S. C., S. MENDES, T. RÉGIS, O. S. PASSOS, W. S. S. FILHO & A. PEDROSA-HARAND. 2019. Cytogenetic map of pummelo and chromosome evolution of true *Citrus* species and the hybrid sweet orange. *J. Agric. Sci.* 11: 148. https://doi.org/10.5539/jas.v11n14p148

SILVESTRI, M .C., A. M. ORTIZ, G. A. R. DOBLADEZ & G. I. LAVIA. 2020. Chromosome diversity in species of the genus *Arachis*, revealed by FISH and CMA/DAPI banding, and inferences about their karyotype differentiation. *An. Acad. Bras. Cienc.* 92: 1–29. https://doi.org/10.1590/0001-3765202020191364

SINGH, R. J. 2003. *Plant cytogenetics*. 3rd ed. Boca Raton, Florida, USA .

SOLTIS, D. E., P. S. SOLTIS, D. W. SCHEMSKE, J. F. HANCOCK, J. N. THOMPSON, B. C. HUSBAND & W. S. JUDD. 2007. Autopolyploidy in angiosperms: have we grossly underestimated the number of species? *Taxon*. 56: 13-30. https://doi.org/10.2307/25065732.

SOUZA, G., A. MARQUES, T. RIBEIRO, L. G. DANTAS, P. ESPERANZA, M GUERRA & O. CROSA. 2019. Allopolyploidy and extensive rDNA site variation underlie rapid karyotype evolution in *Nothoscordum* section *Nothoscordum* (Amaryllidaceae). *Bot. J. Linn. Soc.* 190: 215–228. https://doi.org/10.1093/botlinnean/boz008

STEBBINS, G. L. 1971. *Chromosomal evolution in higher plants*. Edward Arnold Ltd, London.

VAIO, M., J. NASCIMENTO, S. MENDES, A. IBIAPINO, L. P. FÉLIX, A. GARDNER, A. GARDNER, E. EMSHWILLER, P. FIASCHI, M. GUERRA. 2018. Multiple karyotype changes distinguish two closely related species of *Oxalis* (*O. psoraleoides* and *O. rhombeo-ovata*) and suggest an artificial grouping of section *Polymorphae* (Oxalidaceae). *Bot. J. Linn. Soc.* 188: 269–280. https://doi.org/10.1093/botlinnean/boy054

VANZELA, A. L. L., A. A. PAULA, C. C. QUINTAS, T. FERNANDES, J. N. C. BALDISSERA & T. B. SOUZA. 2017. *Cestrum strigilatum* (Ruiz & Pavón, 1799) B chromosome shares repetitive DNA sequences with A chromosomes of different *Cestrum* (Linnaeus, 1753) species. *Comp. Cytogenet.* 11: 511–524. https://doi.org/10.3897/CompCytogen.v11i3.13418